The University of
Nottingham

UNITED KINGDOM · CHINA · MALAYSIA

Simkin, Andrew J. and McAusland, Lorna and Lawson, Tracy and Raines, Christine A. (2017) Overexpression of the RieskeFeS protein increasese electron transport rates and biomass yield. Plant Physiology, 175 . pp. 134-145. ISSN 1532-2548

Access from the University of Nottingham repository:
http://eprints.nottingham.ac.uk/46456/1/2017%20Simkin%20et%20al%20Plant%20Phys%20Rieske.pdf

Copyright and reuse:

A note on versions:

The version presented here may differ from the published version or from the version of record. If you wish to cite this item you are advised to consult the publisher's version. Please see the repository url above for details on accessing the published version and note that access may require a subscription.

For more information, please contact eprints@nottingham.ac.uk

Overexpression of the RieskeFeS Protein Increases Electron Transport Rates and Biomass Yield[1][CC-BY]

Andrew J. Simkin, Lorna McAusland,[2] Tracy Lawson, and Christine A. Raines[3]

School of Biological Sciences, University of Essex, Colchester CO4 3SQ, United Kingdom

ORCID IDs: 0000-0001-5056-1306 (A.J.S.); 0000-0002-5908-1939 (L.M.); 0000-0002-4073-7221 (T.L.); 0000-0001-7997-7823 (C.A.R.).

In this study, we generated transgenic Arabidopsis (*Arabidopsis thaliana*) plants overexpressing the Rieske FeS protein (PetC), a component of the cytochrome b_6f (cyt b_6f) complex. Increasing the levels of this protein resulted in concomitant increases in the levels of cyt f (PetA) and cyt b_6 (PetB), core proteins of the cyt b_6f complex. Interestingly, an increase in the levels of proteins in both the photosystem I (PSI) and PSII complexes also was seen in the Rieske FeS overexpression plants. Although the mechanisms leading to these changes remain to be identified, the transgenic plants presented here provide novel tools to explore this. Importantly, overexpression of the Rieske FeS protein resulted in substantial and significant impacts on the quantum efficiency of PSI and PSII, electron transport, biomass, and seed yield in Arabidopsis plants. These results demonstrate the potential for manipulating electron transport processes to increase crop productivity.

Increasing food and fuel demands by the growing world population has led to the need to develop higher yielding crop varieties (Fischer and Edmeades, 2010; Ray et al., 2012). Transgenic studies, modeling approaches, and theoretical considerations provide evidence that increasing photosynthetic capacity is a viable route to increase the yield of crop plants (Zhu et al., 2010; Raines, 2011; Long et al., 2015; von Caemmerer and Furbank, 2016). There is now a growing body of experimental evidence showing that increasing the levels of photosynthetic enzymes in carbon metabolism results in increased photosynthesis and plant biomass (Miyagawa et al., 2001; Lefebvre et al., 2005; Raines, 2006, 2011; Rosenthal et al., 2011; Uematsu et al., 2012; Simkin et al., 2015, 2017; Driever et al., 2017). In addition, the manipulation of photosynthetic electron transport by the introduction of the algal cytochrome c_6 protein has been shown to improve the efficiency of photosynthesis and to stimulate plant growth in low light (Chida et al., 2007).

One endogenous target identified for manipulation is the cytochrome b_6f (cyt b_6f) complex, which is located in the thylakoid membrane and functions in both linear and cyclic electron transport, providing ATP and NADPH for photosynthetic carbon fixation. Initially, cyt b_6f inhibitors (Kirchhoff et al., 2000), and later, transgenic antisense studies suppressing the accumulation of the Rieske FeS protein (PetC), a component of the cyt b_6f complex, demonstrated that the activity of the cyt b_6f complex is a key determinant of the rate of electron transport (Price et al., 1995, 1998; Anderson et al., 1997; Ruuska et al., 2000; Yamori et al., 2011a, 2011b).

The finding that the cyt b_6f complex is a potential limiting step in the electron transport chain suggests that, by increasing the activity of this complex, it may be possible to increase the rate of photosynthesis. However, questions have been raised about the feasibility of manipulating this multiprotein, membrane-located complex, given that it is composed of eight different subunits, six being encoded in the chloroplast genome (PetA [cyt f], PetB [cyt b_6], PetD, PetG, PetL, and PetN) and two in the nucleus (PetC [Rieske FeS] and PetM; Willey and Gray, 1988; Anderson, 1992; Knight et al., 2002; Cramer and Zhang, 2006; Cramer et al., 2006; Baniulis et al., 2009; Schöttler et al., 2015). Furthermore, this protein complex functions as a dimer, with the transmembrane domains of both the Rieske FeS and cyt b_6 proteins being implicated directly in the monomer-monomer interaction and stability of the complex and the *petD* gene product functioning as a scaffold (Hager et al., 1999; Cramer et al., 2006; Schwenkert et al., 2007; Hojka et al., 2014). Essential roles in the assembly and stability of the cyt b_6f complex also have been shown for the PetG, PetN, and PetM subunits, and a minor role in stability was assigned to the PetL gene product (Bruce and Malkin, 1991; Kuras and Wollman, 1994; Hager et al., 1999; Monde et al., 2000; Schöttler et al., 2007; Schwenkert et al., 2007; Hojka et al., 2014).

Notwithstanding both the genetic and structural complexity of the cyt b_6f complex, it has been shown previously that it is possible to manipulate the levels of the cyt b_6f complex by down-regulation of the expression of the Rieske FeS protein (Price et al., 1998; Yamori et al., 2011b). It also has been shown that the Rieske FeS protein is one of the subunits required for the successful assembly of the cyt b_6f complex (Miles, 1982; Metz et al., 1983; Barkan et al., 1986; Anderson et al., 1997). Based on these results, we reasoned that overexpression of the Rieske FeS protein could be a feasible approach to take in order to increase the electron flow through the cyt b_6f complex. In this article, we report on the production of Arabidopsis (*Arabidopsis thaliana*) with increased levels of the tobacco (*Nicotiana tabacum*) Rieske FeS protein, and we show that this manipulation resulted in increases in photosynthetic electron transport, CO_2 assimilation, and yield. This work provides evidence that the process of electron transport is a potential route for the improvement of plant productivity.

RESULTS

Production and Selection of Rieske FeS Overexpression Transformants

The full-length tobacco Rieske FeS coding sequence (X64353) from the cyt b_6f complex was used to generate an overexpression construct B2-NtRi (Supplemental Fig. S1). Following floral dipping, transgenic Arabidopsis plants were selected on both kanamycin- and hygromycin-containing medium (Nakagawa et al., 2007), and plants expressing the integrated transgenes were identified using reverse transcriptase-PCR (data not shown). Proteins were extracted from leaves of the T1 progeny, allowing the identification of three lines with increased levels of the Rieske FeS protein (PetC; Supplemental Fig. S2A). Immunoblot analysis of T3 progeny of lines 9, 10, and 11 showed them to have higher levels of the Rieske FeS protein when compared with the wild type (Fig. 1; Supplemental Fig. S2B). The overexpression of the Rieske FeS protein (hereafter referred to as Rieske FeS ox) resulted in a concomitant
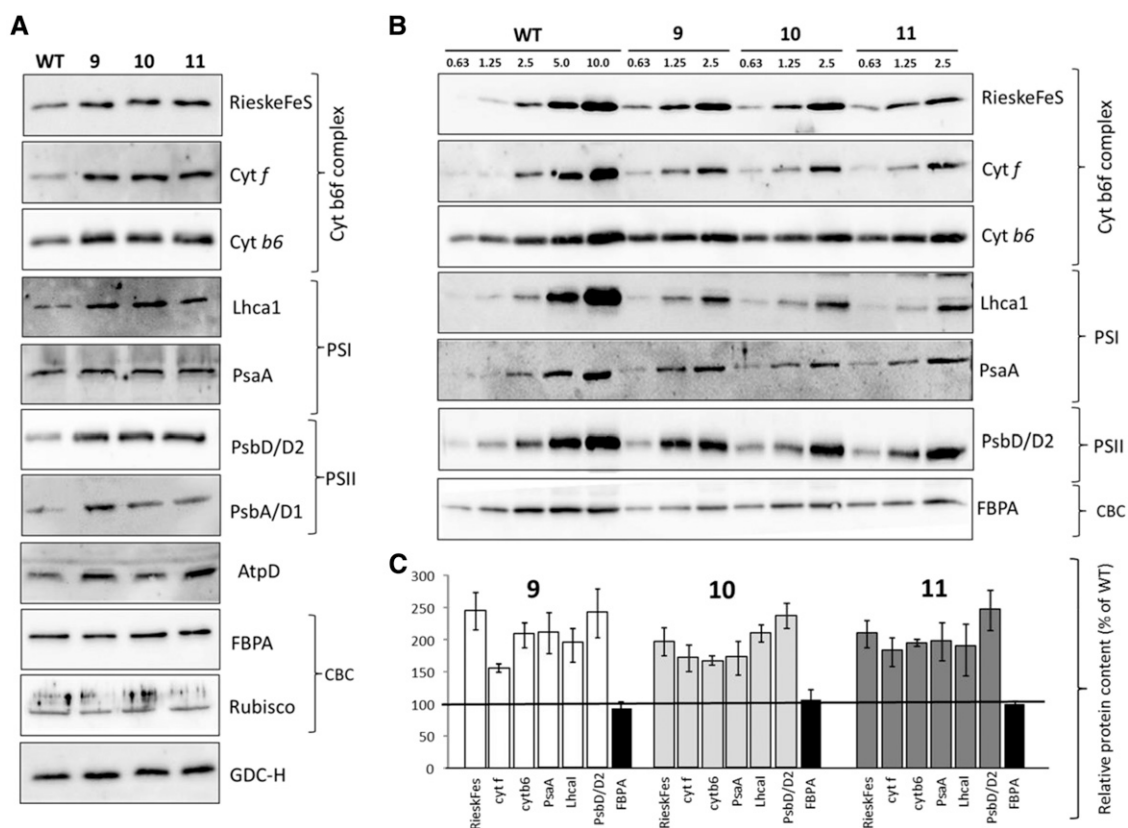
Figure 1. Immunoblot analysis of leaf proteins of wild-type (WT) and Rieske FeS ox plants. Protein extracts were from leaf discs taken from two leaves per plant from three independent lines (9, 10, and 11) and separated on a 12% acrylamide gel, transferred to membranes, and probed with relevant antibodies. The cyt b_6f complex subunits PSI and PSII, ATP synthase δ-subunit (AtpD), Calvin-Benson cycle (CBC) proteins, and photorespiratory GDC-H protein were probed. A, Protein (6 μg) was loaded for all antibodies except for FBPA (3 μg) and Rubisco (1 μg). B, Proteins were loaded containing 0.63 to 10 μg of protein. C, Proteins were quantified using a Fusion FX Vilber Lourmat imager (Peqlab), as described previously (Vialet-Chabrand et al., 2017), and are presented as relative protein contents compared with the wild type.

increase in both cyt f (PetA) and cyt b_6 (PetB; Fig. 1A). An increase in the level of the PSI type I chlorophyll a/b-binding protein (LhcaI) and an increase in the core protein of PSI (PsaA) also were observed. Furthermore, the D1 (PsbA) and D2 (PsbD) proteins, which form the reaction center of PSII, also were shown to be elevated in Rieske FeS ox lines. Finally, an increase in the ATP synthase δ-subunit (AtpD) also was observed in Rieske FeS ox lines (Fig. 1A). In contrast, no notable differences in protein levels for the chloroplastic FBP aldolase (FBPA), the mitochondrial Gly decarboxylase-H protein (GDC-H), or the Rubisco large subunit were observed (Fig. 1A). A quantitative estimate of the changes in protein levels was determined from the immunoblots of leaf extracts isolated from two to three independent plants per line. An example is shown in Figure 1B. These results showed a 2- to 2.5-fold increase in the Rieske FeS protein relative to wild-type plants, and a similar increase also was observed for cyt f, cyt b_6, Lhca1, D2, and PsaA (Fig. 1C). No increase in the stromal FBPA protein was evident.

Chlorophyll Fluorescence Imaging Reveals Increased Photosynthetic Efficiency in Young Rieske FeS ox Seedlings

In order to explore the impact of increased levels of the Rieske FeS protein on photosynthesis, the quantum efficiency of PSII (F_q'/F_m') was analyzed using chlorophyll a fluorescence imaging (Baker, 2008; Murchie and Lawson, 2013). A small increase in F_q'/F_m' was found in the Rieske FeS ox plants at irradiances of 310 and 600 μmol m^{-2} s^{-1} (Fig. 2). Leaf area, generated from these images, was significantly larger in all Rieske FeS ox lines compared with the wild type (Fig. 2C), but no significant difference in leaf thickness was observed between the leaves of Rieske FeS lines 9 and 11 and the wild-type plants (Supplemental Table S1).

Photosynthetic CO$_2$ Assimilation and Electron Transport Rates Are Increased in the Rieske FeS ox Plants

The impact of overexpression of the Rieske FeS protein on the rate of photosynthesis in mature plants was investigated using combined gas-exchange and chlorophyll fluorescence analyses. Both the light-saturated rate of CO$_2$ fixation and the relative light-saturated rate of electron transport (ETRII) were increased in the Rieske FeS ox lines compared with the wild type when measured at 2% [O$_2$] (Fig. 3, A and B; Table I). Additionally, the light-saturated rate of CO$_2$ assimilation at ambient [CO$_2$] also was increased when measured at 21% [O$_2$] (Supplemental Fig. S3). No significant difference in leaf absorbance between the Rieske FeS ox and wild-type plants was found (Supplemental Table S1).

In plants grown at a light level of 130 μmol m^{-2} s^{-1}, no difference in the light- or CO$_2$-saturated rate of CO$_2$ assimilation (A_{max}) was found. In contrast, in a second
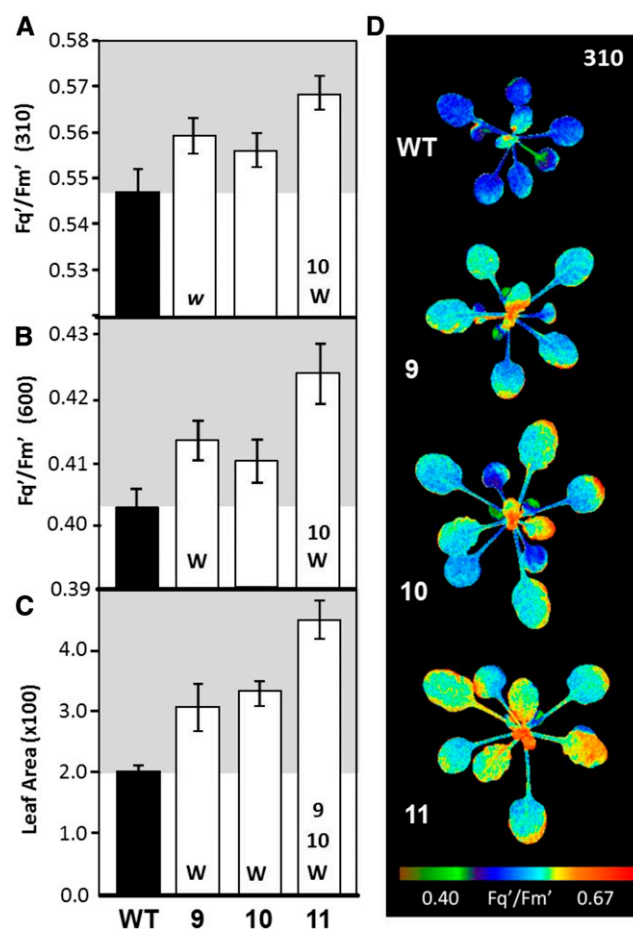

Figure 2. Determination of photosynthetic efficiency and leaf area in Rieske FeS ox seedlings using chlorophyll fluorescence imaging. F_q'/F_m' at 310 μmol m^{-2} s^{-1} (A and D) and 600 μmol m^{-2} s^{-1} (B) and leaf area at the time of analysis (C). The data were obtained using four to six individual plants from each line compared with the wild type (five plants). Significant differences ($P < 0.05$) are represented as uppercase letters indicating differences between lines. Lowercase italic letters indicate lines that are just below significance ($P > 0.05$ and < 0.1). Error bars represent SE. D, Wild type (WT) and Rieske FeS ox plants were grown in controlled-environment conditions with a light intensity of 130 μmol m^{-2} s^{-1}, 8-h-light/16-h-dark cycle, and chlorophyll fluorescence imaging was used to determine F_q'/F_m' at two light intensities 14 d after planting (DAP).

group of plants grown at 280 μmol m^{-2} s^{-1}, A_{max} was greater in the Rieske FeS ox lines 9 and 11 relative to the wild type (Fig. 3C; Table I). Further analysis of the A/C_i curves revealed that maximum electron transport rate was significantly greater in the Rieske FeS ox plants when compared with the wild type (Table II), but no significant difference in the maximum rate of Rubisco (data not shown) was observed.

The Quantum Efficiency of PSI and PSII Was Increased in the Rieske FeS ox Plants

To further explore the influence of increases in the Rieske FeS protein on PSII and PSI photochemistry, dark-light
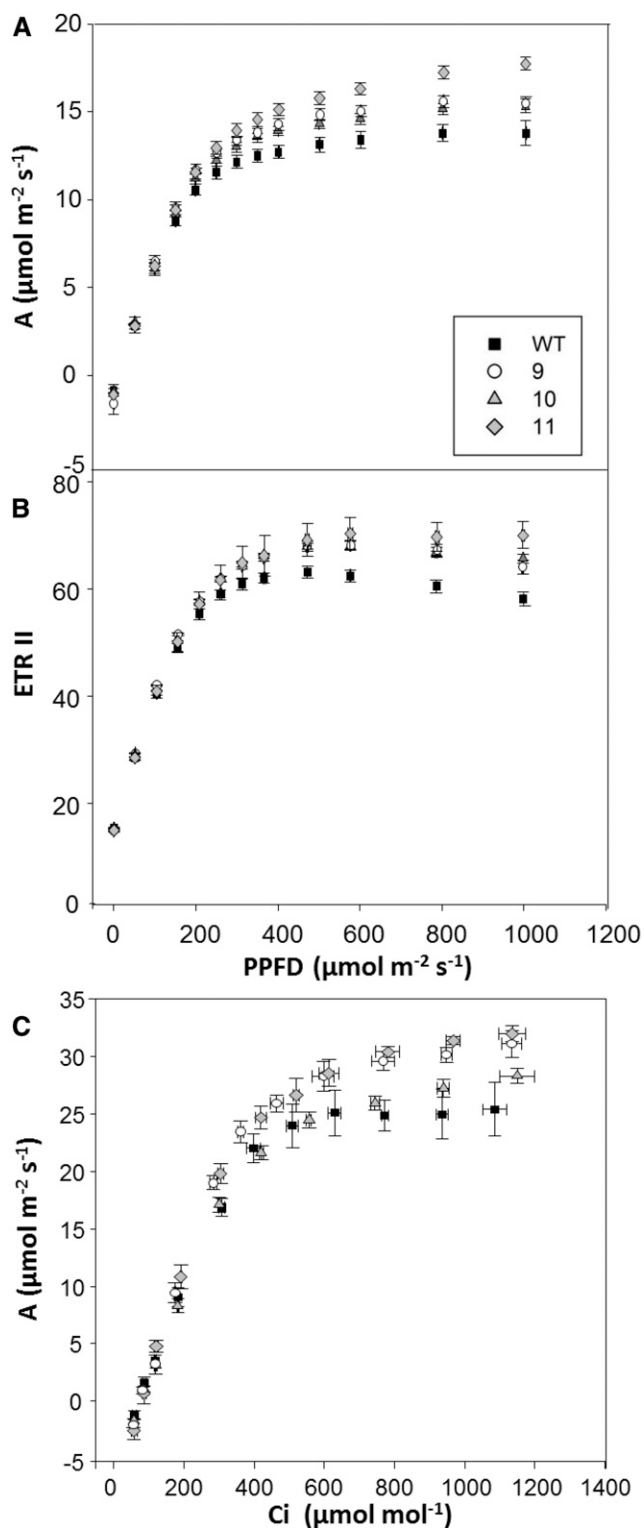
Figure 3. Photosynthetic responses of the Rieske FeS ox plants. A and B, Determination of photosynthetic capacity (A) and electron transport rates (B) in transgenic plants at 2% [O_2]. Wild-type (WT) and transgenic plants were grown in controlled-environment conditions with a light intensity 130 μmol m^{-2} s^{-1} and an 8-h-light/16-h-dark cycle for 4 weeks. C, Photosynthetic carbon fixation rate (A) was determined as a function of increasing CO_2 concentrations (A/C_i) at saturating light

induction responses were determined in the wild type and Rieske FeS ox (lines 11 and 10) using simultaneous measurements of P700 oxidation state and PSII efficiency. These results showed that the quantum yields of both PSI and PSII were increased in the Rieske FeS ox plants compared with the wild type and that the fraction of PSII centers that were open (q_L) also was increased, while the level of Qa reduction ($1 − q_p$) was lower in leaves of 27-d-old plants from line 11 (Fig. 4). non-photochemical quenching (NPQ) levels also were shown to be lower in the Rieske FeS ox plants, together with a reduction in stress-induced limitation of NPQ (q_N) when compared with wild-type plants (Fig. 4). Similar results were obtained for both lines 10 and 11 when plants were analyzed later in development (34 DAP; Supplemental Fig. S4). The increases in the quantum yields of PSI and PSII observed here were accompanied by corresponding increases in electron transport rates (ETRI and ETRII; Supplemental Fig. S5, A and D); however, a bigger increase in ETRII relative to ETRI was observed, demonstrated by the wild type having a higher ETRI-ETRII ratio (Supplemental Fig. S5, C and D).

Growth, Vegetative Biomass, and Seed Yield Are Increased in the Rieske FeS ox Plants

The leaf area of the Rieske FeS ox lines was significantly greater than that of the wild type as early as 10 DAP in soil, and by 18 d it was 40% to 114% larger (Fig. 5). Destructive harvest at day 25 showed that this increase in leaf area translated to an increase in shoot biomass of between 29% and 72% determined as dry weight (Fig. 5C). To determine the impact of increased Rieske FeS protein on seed yield and final shoot biomass, a second group of plants was grown in the same conditions as described in Figure 6. Interestingly, at 38 DAP, 40% of the Rieske FeS ox plants had flowered, in contrast to 22% in the wild-type plants (Fig. 6A). Following seed set (52 DAP), both vegetative biomass (Fig. 6B) and seed yield (Fig. 6C) were determined, and although a significant increase in biomass was observed in all of the Rieske FeS ox plants, a statistically significant increase in seed yield was evident only in line 11.

Pigment Content Was Altered in the Rieske FeS ox Plants

The pigment composition of the leaves of the Rieske FeS ox and wild-type plants was determined. Increases in the levels of chlorophyll *a* and *b* (14%–29%) were observed in the Rieske FeS ox compared with wild-type

levels (1,000 μmol m^{-2} s^{-1}). Wild-type and transgenic plants were grown in controlled-environment conditions at a light intensity 280 μmol m^{-2} s^{-1} and a 12-h-light/12-h-dark cycle for 4 weeks. Error bars represent SE.

Table I. *Photosynthetic parameters of wild-type and Rieske FeS ox lines determined from light response curves carried out at 2% [O_2] (see Fig. 3, A and B)*

Statistical differences are shown in boldface (* $P < 0.1$; ** $P < 0.05$; and *** $P < 0.01$). A_{sat}, Light-saturated rate of CO_2 fixation. SE values are shown.

Name	Parameters				
	Light	F_q'/F_m'	ETRII	q_P	A_{sat}
	$\mu mol\ m^{-2}\ s^{-1}$		$\mu mol\ e^-\ m^{-2}\ s^{-1}$		$\mu mol\ m^{-2}\ s^{-1}$
Wild type	400	0.343 ± 0.013	62.3 ± 0.96	0.58 ± 0.02	14.7 ± 0.35
	1,000	0.124 ± 0.002	54.4 ± 0.91	0.23 ± 0.01	
9	400	**0.380 ± 0.004****	**66.5 ± 0.46****	**0.64 ± 0.00****	**16.5 ± 0.13****
	1,000	**0.151 ± 0.002*****	**65.9 ± 0.79*****	**0.28 ± 0.00****	
10	400	0.369 ± 0.009	**65.9 ± 0.68****	0.62 ± 0.01	**17.7 ± 0.87*****
	1,000	**0.147 ± 0.003*****	**64.3 ± 1.24*****	**0.27 ± 0.00***	
11	400	0.370 ± 0.018	66.4 ± 3.73	0.63 ± 0.02	**18.4 ± 0.44*****
	1,000	**0.156 ± 0.006*****	**70.3 ± 2.47*****	**0.29 ± 0.00*****	

plants (Fig. 7). Plants with increased Rieske FeS protein also were found to have a small increase in the chlorophyll *a/b* ratio, from 2.96 to 3.12. These increases were accompanied by increases in the carotenoids, neoxanthin (+38%), violaxanthin (+59%), lutein (+75%), and β-carotene (+169%). No detectable change in the level of zeaxanthin was evident in the Rieske FeS ox plants. The increases in both total chlorophyll and total carotenoids also led to a significant decrease in the chlorophyll-to-carotenoid ratio, from 3.6 to 2.4 (Fig. 7).

DISCUSSION

In recent years, increasing the rate of photosynthetic carbon assimilation has been identified as a target for improvement to increase yield. Evidence to support this has come from the theory and modeling of the photosynthetic process, growth of plants in elevated CO_2, and transgenic manipulation (Zhu et al., 2010). It was shown previously in antisense studies that reducing the levels of the Rieske FeS protein resulted in a reduction in levels of the cyt b_6f complex, a decrease in photosynthetic electron transport, and, in rice (*Oryza sativa*), a decrease in both biomass and seed yield (Price et al., 1998; Yamori et al., 2016). These findings identified the cyt b_6f complex as a limiting step in electron transport and would suggest that overexpression of the Rieske FeS protein may be a feasible route to increase photosynthesis and yield. In this study, we show that overexpression of the Rieske FeS protein in Arabidopsis results in increases in photosynthesis, vegetative biomass, and seed yield.

Increased Levels of the Rieske FeS Protein Increased Photosynthetic Electron Transport, CO_2 Assimilation, and Biomass

Using chlorophyll fluorescence imaging, we have shown that overexpression of the Rieske FeS protein resulted in increases in photosynthesis and growth, which are evident from the early stages of seedling development. These observed increases in F_q'/F_m' represent an early indication that the potential quantum yield of PSII photochemistry had been elevated in Rieske FeS ox lines (Genty et al., 1989, 1992; Baker et al., 2007). This early stimulation is maintained into maturity, and increases in the light-saturated rate of CO_2 assimilation and electron transport rates were evident in the Rieske FeS ox plants. Our data also showed that quantum yields of both PSII and PSI were increased and that the fraction of PSII centers available for photochemistry was increased, as indicated by an increase in q_L and a lower $1 - q_p$ (Baker and Oxborough, 2004; Kramer et al., 2004; Baker et al., 2007). These results are consistent with what would be predicted from results obtained from the Rieske FeS antisense studies where ETR was reduced (Price et al., 1998; Ruuska et al., 2000; Yamori et al., 2011b). However, the impact of overexpression of the Rieske FeS protein was clearly not restricted to increasing the activity of the cyt b_6/f complex but resulted in changes in PSI, PSII, and the ATPase complex, which led to an increase in electron flow through the entire electron transport chain. Analysis of the ratio of PSI to PSII electron transport showed that, relative to wild-type plants, the Rieske ox lines have higher rates of PSII ETR relative to PSI, which may be related to cyclic electron flow, differences in energy distribution, and/or the PSI-PSII ratio (Kono et al., 2014).

In addition to increased rates of photosynthesis, a substantial and significant increase in the growth of the

Table II. *Maximum electron transport rate (J_{max}) and maximum assimilation (A_{max}) in wild-type and Rieske FeS ox lines*

Results were derived from the A/C_i response curves shown in Figure 3C using the equations published by von Caemmerer and Farquhar (1981). Statistical differences are shown in boldface (* $P < 0.1$ and ** $P < 0.05$). SE values are shown.

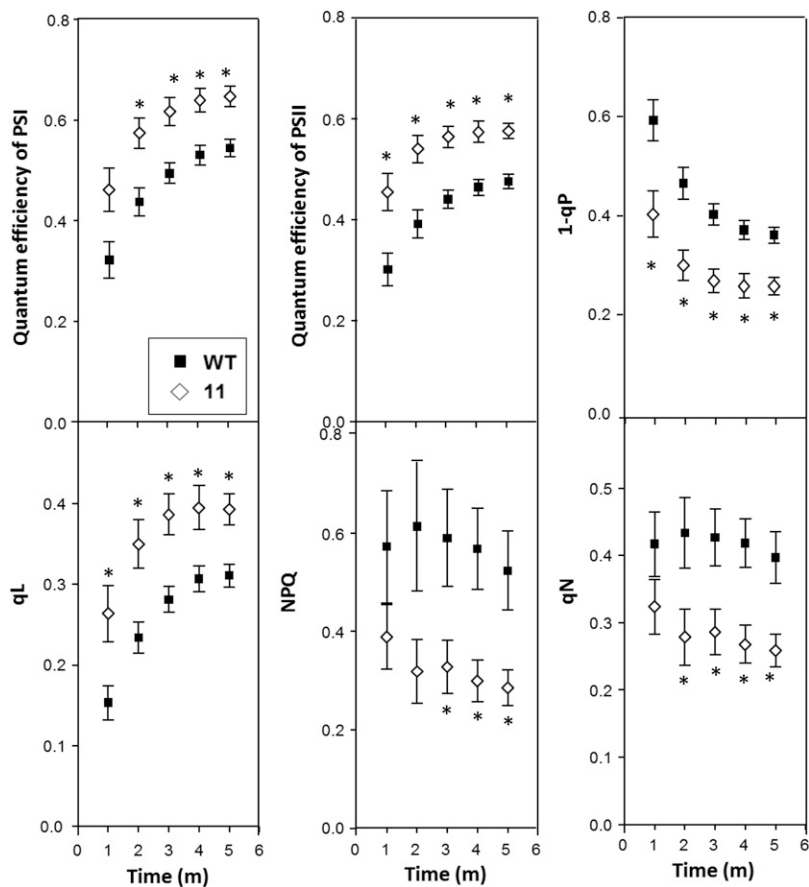| Name	Parameters	
	J_{max} ($\mu mol\ m^{-2}\ s^{-1}$)	A_{max} ($\mu mol\ m^{-2}\ s^{-1}$)
Wild type	181 ± 11.6	24.4 ± 2.31
9	**210 ± 10.2***	**31.1 ± 1.14***
10	194 ± 8.9	28.3 ± 0.67
11	**216 ± 11.9***	**31.9 ± 0.68***

Figure 4. Determination of the efficiency of electron transport in leaves of young Rieske FeS ox plants. Wild-type (WT) and Rieske FeS ox plants were grown in controlled-environment conditions with a light intensity of 130 mmol m^{-2} s^{-1} and an 8-h-light/16-h-dark cycle, and the redox state was determined (27 DAP) using a Dual-PAM instrument at a light intensity of 220 μmol m^{-2} s^{-1}. The data were obtained using four individual plants from Rieske FeS ox line 11 compared with the wild type (five plants). Significant differences are indicated (*, $P < 0.05$). Error bars represent SE.

rosette area was observed in the Rieske FeS ox plants in the early vegetative phase, which resulted in an approximately 30% to 70% increase in biomass yield in the different lines. Importantly, seed yields in line 11, which showed the biggest increases in shoot biomass, also were

shown to be increased relative to the wild type. Given that increases in leaf area are evident in the Rieske ox plants from early in development, the improvements in biomass are likely due to a combination of increased light capture and photosynthesis due to the greater leaf area.
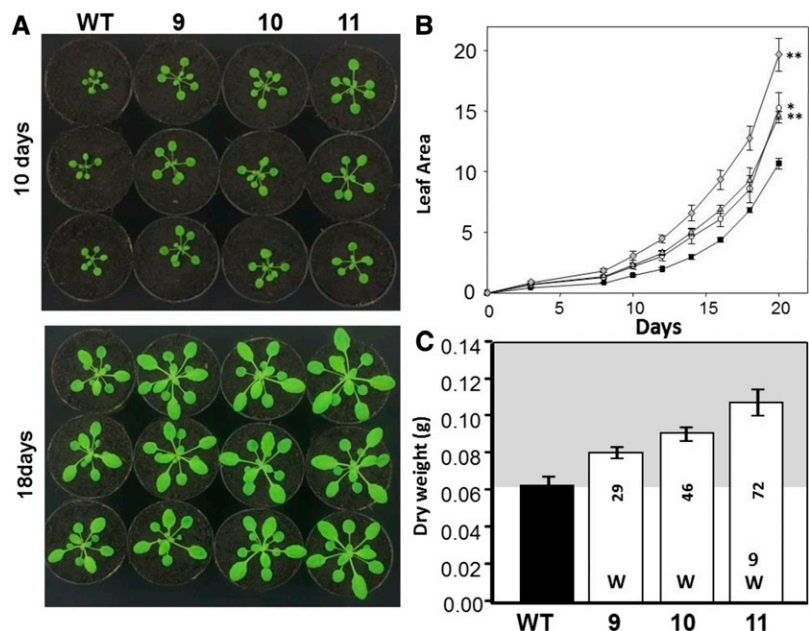

Figure 5. Growth analysis of wild-type (WT) and Rieske FeS ox plants. Plants were grown at 130 μmol m^{-2} s^{-1} light intensity in short days (8 h of light/16 h of dark). A, Appearance of plants at 10 and 18 DAP. B, Leaf area determined at 20 DAP. Significant differences (*, $P < 0.01$ and **, $P < 0.001$) are indicated. C, Final biomass at 25 DAP. Results are representative of six to nine plants from each line. Increase over wild type (%) is indicated as numbers on the histogram. Significant differences ($P < 0.05$) are represented by uppercase letters. Error bars represent SE.
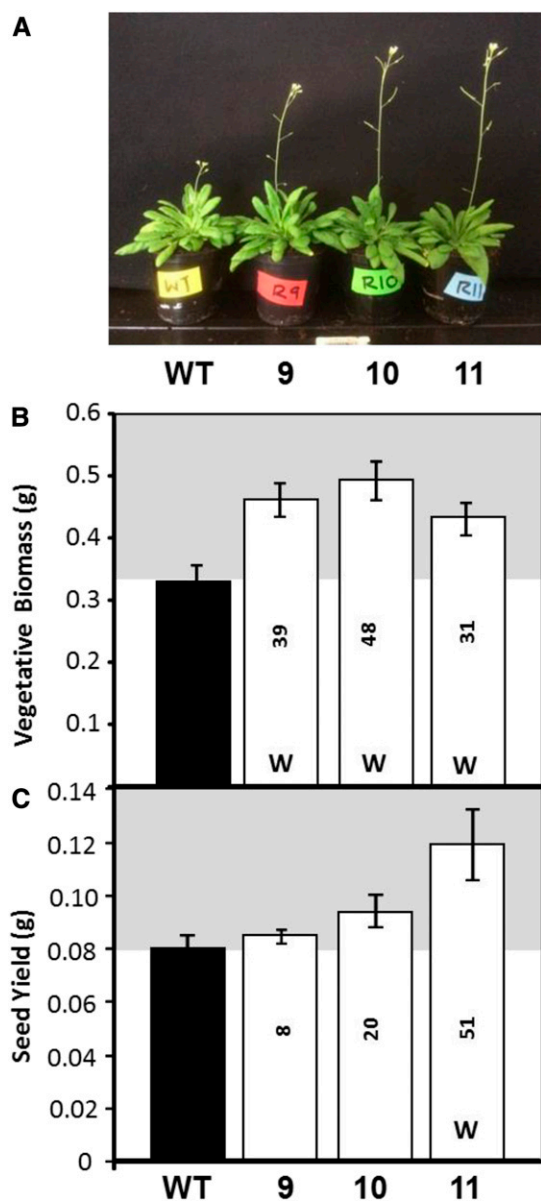
Figure 6. Seed yield and vegetative biomass of wild-type (WT) and Rieske FeS ox plants. Plants were grown at 130 μmol m^{-2} s^{-1} light intensity in short days (8 h of light/16 h of dark). A, Appearance of plants at 38 DAP. B and C, Final biomass (B) and seed yield at harvest (52 DAP; C). Increase over the wild type (%) is indicated by numbers on the histograms. Results are representative of six to nine plants from each line. Significant differences ($P < 0.05$) are represented by uppercase letters. Error bars represent SE.

Rieske FeS ox Plants Have Increased Levels of Proteins in the cyt b_6f, PSI, and PSII Complexes

In keeping with our analysis of the electron transport processes in the Rieske FeS ox plants, increases in the levels of cyt b_6 and cyt f, core proteins of the cyt b_6f complex, were evident. Furthermore, increases in the levels of proteins in both PSII and PS1 and the δ-subunit of the ATPase complex also were observed. This result

was unexpected, given that no changes in the components of PSII or PSI were observed in the Rieske FeS antisense plants. In contrast, in keeping with this study, the *hcf* mutant, in which the biogenesis of the cyt b_6f complex was inhibited, also had a reduced accumulation of components of both PSI and PSII (Lennartz et al., 2001). In addition, a recent study reported increases in cyt b_6f protein levels in Arabidopsis plants grown under square-wave light compared with plants grown under fluctuating light, and these were accompanied by increased levels of PSII, PSI, and the δ-subunit of the ATPase proteins (Vialet-Chabrand et al., 2017). Taken together, these results provide further demonstration of the ability of the thylakoid membrane to respond to changes in the external and internal environments (Foyer et al., 2012). Although there are many examples of coordination of the accumulation of photosynthetic complexes in the thylakoid membrane, the underlying regulation of the synthesis and assembly of components of the thylakoid membrane, the factors determining the accumulation of these complexes, is still poorly understood (Schöttler et al., 2015). Recently, a nucleus-encoded chloroplast RNA-binding protein, photosystem biogenesis regulator1 (PBR1), was identified and shown to be involved in the coordination of the biogenesis of the PSI, cyt b_6f, and NDH complexes (Yang et al., 2016). It will be interesting to explore the role of PBR1 in the plants produced in this study, as these are likely useful tools to investigate fundamental questions on factors controlling both the biogenesis and activities of the photosynthetic complexes in the electron transport chain.

A recent study has shown that, for rice plants growing in elevated CO_2, a small decrease in Rubisco protein levels resulted in an increase in the electron transport components and an increase in biomass (Kanno et al., 2017). Given the increase in thylakoid protein composition of the Rieske ox plants, it might be expected that there would be some tradeoff, and a reduction in other proteins may occur to compensate. Although no comprehensive analysis of proteins has been undertaken in these plants, we found no evidence of changes in the levels of Rubisco, which is a major N sink or FBPA and GDC. What is not yet clear is the impact of this manipulation on nitrogen use efficiency (NUE), and a full analysis of the performance of these plants under different N regimes will be needed to explore this question.

Overexpression of Rieske FeS Significantly Modifies the Pigment Content of Leaves

In parallel with the increase in components of the thylakoid membranes, plants with increased Rieske FeS protein were found to have increases in the levels of both chlorophyll *a* and *b* and a small increase in the chlorophyll *a/b* ratio, from 2.96 to 3.12. The increases in chlorophyll *a* and *b* suggest a greater investment in both light capture and PSII reaction centers and would fit with the increase in photosynthetic electron transport
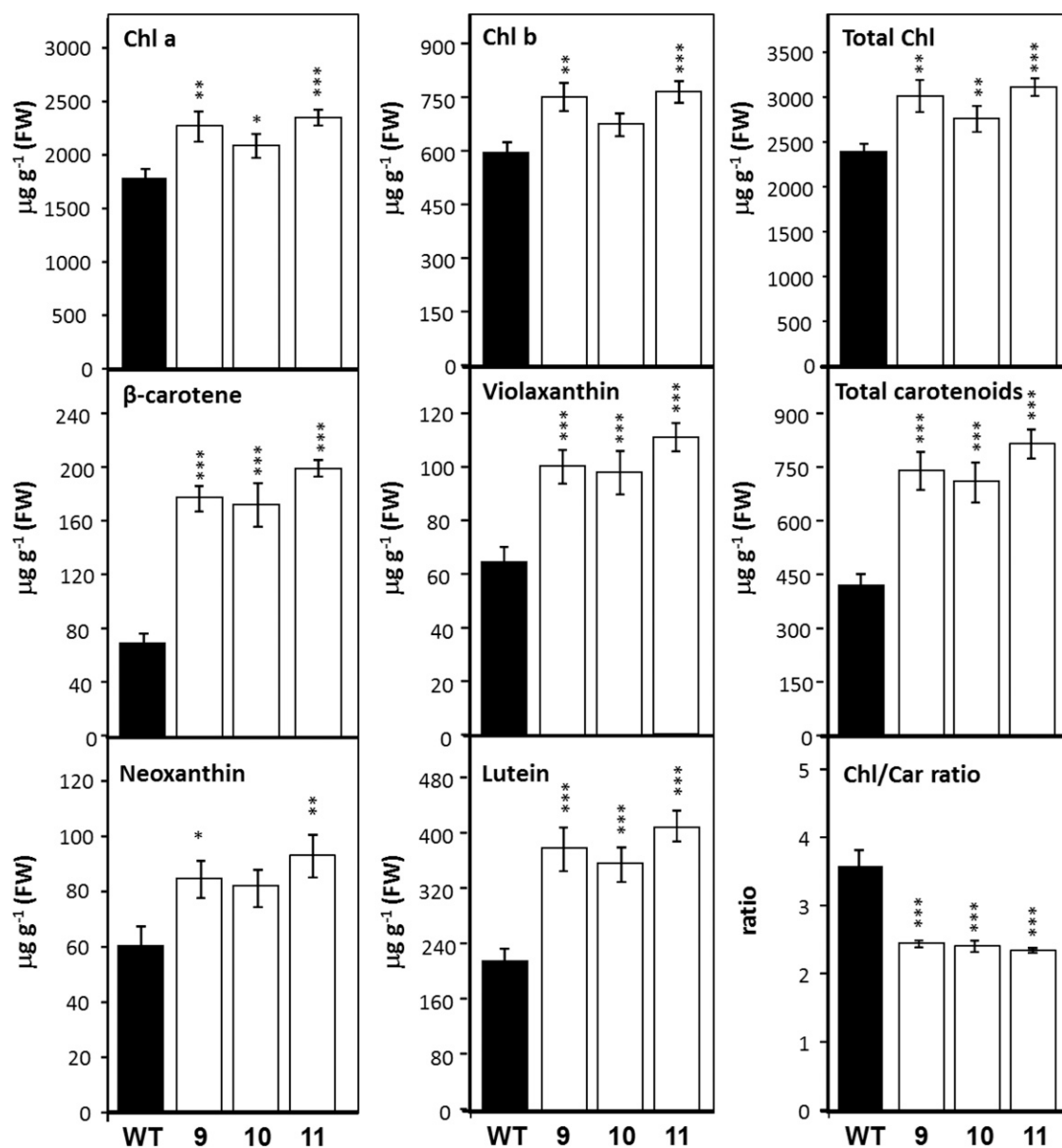
Figure 7. Pigment content in wild-type (WT) and Rieske FeS ox plants. Plants were grown at 130 μmol m^{-2} s^{-1} light intensity in short days (8 h of light/16 h of dark). Two leaf discs, collected from two different leaves, were immersed in *N,N*-dimethylformamide (DMF) at 4°C for 48 h and separated by ultra-performance liquid chromatography. Results are represented as μg g^{-1} fresh weight (FW). Statistical differences are shown by asterisks (*, $P < 0.1$; **, $P < 0.05$; and ***, $P < 0.001$). Error bars represent SE.

capacity in the Rieske FeS ox plants. In previous work, plants with reduced levels of the Rieske FeS protein had a lower chlorophyll *a/b* ratio (Hurry et al., 1996; Price et al., 1998), which is the opposite of what was observed in the Rieske FeS ox plants. In addition to increases in chlorophyll, significant increases in the carotenoid pigments also were seen with β-carotene (+169%), violaxanthin (+59%), lutein (+75%), and neoxanthin (+37%). β-Carotene is a component of both the reaction centers (RC) and light-harvesting complex (Kamiya and Shen, 2003; Ferreira et al., 2004; Loll et al., 2005; Litvin et al., 2008; Janik et al., 2016), and the increase in these pigments observed in the

Rieske FeS ox plants is in agreement with the investment in both light harvesting and increasing RC efficiency. We also observed a significant decrease in the chlorophyll-to-carotenoid ratio in Rieske FeS ox plants, which would suggest that there is a greater investment in photoprotection relative to the increased chlorophyll for light harvesting. This increase in carotenoids relative to chlorophyll may contribute to the lower NPQ observed in Rieske FeS ox plants (Kaňa et al., 2016).

Lutein, neoxanthin, and violaxanthin are the main xanthophyll pigment constituents of the largest light-harvesting pigment-protein complex of photosystem II

Simkin et al.

(Thayer and Björkman, 1992; Ruban et al., 1994, 1996, 1999; Ruban, 2012; Janik et al., 2016). Acidification of the thylakoid lumen as a result of electron transport (and driven in particular by the activities of the cyt b_6f complex) is accompanied by the deepoxidation of violaxanthin and an accumulation of zeaxanthin (Björkman and Demmig-Adams, 1994; Müller et al., 2001; Ruban, 2012) as well as protonation of carboxylic acid residues of the PsbS protein associated with PSII antennae (Li et al., 2000, 2004). Protonation of PsbS and binding of zeaxanthin increase NPQ and the thermal dissipation of excitation energy (Baker, 2008; Jahns and Holzwarth, 2012). However, we found that the increase in the level of the Rieske FeS protein led to small but significantly lower steady-state levels of NPQ. The absence of an increase in NPQ in the presence of significant increases in electron transport rates suggests that the Rieske FeS ox plants also have increased rates of ATP synthesis. Although we provide no direct support for this, we did observe an increase in the level of the ATP synthase δ-subunit protein in the Rieske FeS ox plants. Further support for this suggestion comes from earlier work on Rieske FeS antisense plants, which showed that the level of ATP synthase and the transthylakoid pH gradient were both reduced (Price et al., 1995, 1998; Ruuska et al., 2000).

CONCLUSION

A number of studies have shown that increasing photosynthesis through the manipulation of CO_2 assimilation can improve growth (Miyagawa et al., 2001; Lefebvre et al., 2005; Rosenthal et al., 2011; Uematsu et al., 2012; Simkin et al., 2015, 2017). This work, together with a study in which cytochrome c_6 from the red alga *Porphyra* was expressed in Arabidopsis (Chida et al., 2007), provides direct evidence that there is also an opportunity to improve the efficiency of the electron transfer chain. Here, we have shown not only that overexpression of the Rieske FeS protein resulted in increases in cyt f and cyt b_6 proteins of the cyt b_6f complex but that components of PSI, PSII, and the ATPase also were increased. Under the conditions of growth used in this study, these changes led to improvements in photosynthesis and biomass obtained from the Rieske ox plants relative to the wild type.

MATERIALS AND METHODS

Rieske FeS Protein of cyt b_6f

The full-length coding sequence of the Rieske FeS protein of the cyt b_6f (X64353) complex was amplified by reverse transcription-PCR using primers NtRieskeFeSF (5'-caccATGGCTTCTTCTACTCTTTCTCCAG-3') and NtRieskeFeSR (5'-CTAAGCCCACCATGGATCTTCACC-3'). The resulting amplified product was cloned into pENTR/D (Invitrogen) to make pENTR-*NtRieskeFeS*, and the sequence was verified and found to be identical. The full-length cDNA was introduced into the pGWB2 Gateway vector (Nakagawa et al., 2007; AB289765) by recombination from the pENTR/D vector to make pGW-NtRieske (B2-NtRi). cDNAs are under transcriptional control of the 35S tobacco mosaic

virus promoter, which directs constitutive high-level transcription of the transgene, followed by the *nos* 3' terminator. Full details of the B2-NtRi construct assembly can be seen in Supplemental Figure S1.

Generation of Transgenic Plants

The recombinant plasmid B2-NtRi was introduced into wild-type Arabidopsis (*Arabidopsis thaliana*) by floral dipping (Clough and Bent, 1998) using *Agrobacterium tumefaciens* GV3101. Positive transformants were regenerated on Murashige and Skoog medium containing kanamycin (50 mg L^{-1}) and hygromycin (20 mg L^{-1}). Kanamycin/hygromycin-resistant primary transformants (T1 generation) with established root systems were transferred to soil and allowed to self-fertilize.

Plant Growth Conditions

Wild-type T2 Arabidopsis plants resulting from self-fertilization of transgenic plants were germinated in sterile agar medium containing Murashige and Skoog salts, selected on kanamycin, grown to seed in soil (Levington F2; Fisons), and lines of interest were identified by western blot and quantitative PCR. For experimental study, T3 progeny seeds from selected lines were germinated on soil in controlled-environment chambers at an irradiance of 130 μmol m^{-2} s^{-1} in an 8-h/16-h square-wave photoperiod with an air temperature of 22°C and a relative humidity of 60%. Plant position was randomized, and the position of the trays was rotated daily under the light. Leaf areas were calculated from photographic images using ImageJ software (imagej.nih.gov/ij). Wild-type plants used in this study were a combined group of the wild type and null segregants from the transgenic lines, verified by PCR for nonintegration of the transgene, as no significant differences in growth parameters were seen between them (Supplemental Fig. S2).

Protein Extraction and Immunoblotting

Four leaf discs (0.6 cm diameter) from two individual leaves were taken, immediately plunged into liquid N$_2$, and subsequently stored at −80°C. Samples were ground in liquid nitrogen, and protein quantification was determined (Harrison et al., 1998). Samples were loaded on an equal protein basis, separated using 12% (w/v) SDS-PAGE, transferred to a polyvinylidene difluoride membrane, and probed using antibodies raised against the cyt b_6f complex proteins cyt f (PetA; AS08306), cyt b_6 (PetB; AS03034), Rieske FeS (PetC; AS08330), the PSI Lhca1 (AS01005) and PsaA (AS06172) proteins, the PSII PsbA/D1 (AS01016) and PsbD/D2 (AS06146) proteins, the ATP synthase δ-subunit (AS101591), and the Gly decarboxylase H-subunit (AS05074), all purchased from Agrisera (via Newmarket Scientific). FBPA antibodies were raised against a peptide from a conserved region of the protein [C]-ASIGLENTEANRQAYR-amide (Cambridge Research Biochemicals; Simkin et al., 2015). Proteins were detected using horseradish peroxidase conjugated to the secondary antibody and ECL chemiluminescence detection reagent (Amersham). Proteins were quantified using a Fusion FX Vilber Lourmat imager (Peqlab), as described previously (Vialet-Chabrand et al., 2017).

Chlorophyll Fluorescence Imaging

Chlorophyll fluorescence measurements were performed on 10-d-old Arabidopsis seedlings that had been grown in a controlled-environment chamber at a photosynthetic photon flux density (PPFD) of 130 μmol m^{-2} s^{-1} with ambient CO_2 at 22°C. Images of the operating efficiency of PSII photochemistry (F_q'/F_m') were taken at PPFDs of 310 and 600 μmol m^{-2} s^{-1} using a chlorophyll fluorescence imaging system (Technologica; Barbagallo et al., 2003; Baker and Rosenqvist, 2004). F_q'/F_m', was calculated from measurements of steady-state fluorescence in the light (F'), and maximum fluorescence in the light (F_m') was obtained after a saturating 800-ms pulse of 6,200 μmol m^{-2} s^{-1} PPFD using the following equation: $F_q'/F_m' = (F_m' - F')/F_m'$ (Oxborough and Baker 1997a; Baker et al., 2001).

A/C_i Response Curves

The response of A to C_i was measured using a portable gas-exchange system (CIRAS-1; PP Systems). Leaves were illuminated using a red-blue light source attached to the gas-exchange system, and light levels were maintained at saturating PPFD of 1,000 μmol m^{-2} s^{-1} with an integral light-emitting diode light

source (PP Systems) for the duration of the A/C_i response curve. Measurements of A were made at ambient CO_2 concentration (C_a) of 400 μmol mol^{-1}, before C_a was decreased in a stepwise manner to 300, 200, 150, 100, and 50 μmol mol^{-1} before returning to the initial value and increased to 500, 600, 700, 800, 900, 1,000, 1,100, and 1,200 μmol mol^{-1}. Leaf temperature and vapor pressure deficit were maintained at 22°C and 1 ± 0.2 kPa, respectively. The maximum rate of Rubisco and the maximum rate of electron transport for ribulose 1,5-bisphosphate regeneration were determined and standardized to a leaf temperature of 25°C based on equations from Bernacchi et al. (2001) and McMurtrie and Wang (1993), respectively.

Photosynthetic Capacity

Photosynthesis as a function of PPFD (A/Q response curves) was measured using the 6400XT portable gas-exchange system (Li-Cor). Cuvette conditions were maintained at a leaf temperature of 22°C, relative humidity of 50% to 60%, and ambient growth CO_2 concentration of 400 μmol mol^{-1} for plants grown in ambient conditions. Leaves were initially stabilized at saturating irradiance of 1,000 μmol m^{-2} s^{-1}, after which A and stomatal conductance were measured at the following PPFD levels: 0, 50, 100, 150, 200, 250, 300, 350, 400, 500, 600, 800, and 1,000 μmol m^{-2} s^{-1}. Measurements were recorded after A reached a new steady state (1−3 min) and before stomatal conductance changed to the new light levels. A/Q analyses were performed at 21% and 2% [O_2].

PSI and PSII Quantum Efficiency

The photochemical quantum efficiency of PSII and PSI in transgenic and wild-type plants was measured following a dark-light induction transition using a Dual-PAM-100 instrument (Walz) with a DUAL-DR measuring head. Plants were dark adapted for 20 min before placing in the instrument. Following a dark-adapted measurement, plants were illuminated with 220 μmol m^{-2} s^{-1} PPFD. The maximum quantum yield of PSII was measured following a saturating pulse of light for 600 ms at an intensity of 6,200 μmol m^{-2} s^{-1}. The PSII operating efficiency was determined as described by the routines above. PSI quantum efficiency was measured as an absorption change of P700 before and after a saturating pulse of 6,200 μmol m^{-2} s^{-1} for 300 ms (which fully oxidizes P700) in the presence of far-red light with a far-red preillumination of 10 s. Both measurements were recorded every 1 min for 5 min. q_p or F_v'/F_m' was calculated from measurements of steady-state fluorescence in the light (F') and maximum fluorescence in the light (F_m'), while minimal fluorescence in the light (F_o') was calculated following the equation of Oxborough and Baker (1997b). The fraction of open PSII centers (q_L) was calculated from $q_p \times F_o'/F$ (Baker, 2008).

Pigment Extraction and HPLC Analysis

Chlorophylls and carotenoids were extracted using DMF as described previously (Inskeep and Bloom, 1985), which was shown subsequently to suppress chlorophyllide formation in Arabidopsis leaves (Hu et al., 2013). Briefly, two leaf discs collected from two different leaves were immersed in DMF at 4°C for 48 h and separated by ultra-performance liquid chromatography as described by Zapata et al. (2000).

Leaf Thickness

Leaves of equivalent developmental stage were collected from plants after 28 d of growth. Strips were cut from the center of the leaf, avoiding the midvein, preserved in 5% glutaraldehyde, stored at 4°C for 24 h, followed by dehydration in sequential ethanol solutions of 20%, 40%, 80%, and 100% (v/v). The samples were placed in LR White acrylic resin (Sigma-Aldrich), refrigerated for 24 h, embedded in capsules, and placed at 60°C for 24 h. Sections (0.5 μm) were cut using a Reichert-Jung Ultracut microtome (Ametek), fixed, stained, and viewed with a light microscope (López-Juez et al., 1998). Leaf thickness was determined by measuring leaves from two to three plants from lines 9 and 11 compared with leaves from four wild-type plants.

Statistical Analysis

All statistical analyses were done by comparing ANOVA using Sys-stat (University of Essex). The differences between means were tested using the posthoc Tukey's test (SPSS).

Accession Numbers

Sequence data from this article can be found in the GenBank/EMBL data libraries under accession number X64353.

Supplemental Data

The following supplemental materials are available.

Supplemental Figure S1. Schematic representation of the Rieske FeS over-expression vector pGWRi used to transform Arabidopsis.

Supplemental Figure S2. Determination of photosynthetic efficiency and leaf area of the wild type versus azygous segregating controls using chlorophyll fluorescence imaging.

Supplemental Figure S3. Immunoblot analysis of wild-type and Rieske FeS ox proteins.

Supplemental Figure S4. Light response curves of the Rieske FeS plants at 21% [O_2].

Supplemental Figure S5. Determination of the efficiency of electron transport in leaves of mature Rieske FeS ox plants.

Supplemental Figure S6. Determination of the efficiency of electron transport in leaves of young and mature Rieske FeS ox plants.

Supplemental Table S1. Physiological parameters of Rieske FeS ox plants compared with the wild type.

LITERATURE CITED

Anderson JM (1992) Cytochrome b 6 f complex: dynamic molecular organization, function and acclimation. Photosynth Res **34:** 341–357

Anderson JM, Price GD, Chow WS, Hope AB, Badger MR (1997) Reduced levels of cytochrome bf complex in transgenic tobacco leads to marked photochemical reduction of the plastoquinone pool, without significant change in acclimation to irradiance. Photosynth Res **53:** 215–227

Baker NR (2008) Chlorophyll fluorescence: a probe of photosynthesis in vivo. Annu Rev Plant Biol **59:** 89–113

Baker NR, Harbinson J, Kramer DM (2007) Determining the limitations and regulation of photosynthetic energy transduction in leaves. Plant Cell Environ **30:** 1107–1125

Baker NR, Oxborough K (2004) Chlorophyll fluorescence as a probe of photosynthetic productivity. In GC Papageorgiou and Govindjee, eds, Chlorophyll a Fluorescence: A Signature of Photosynthesis, Springer, Dordrecht, the Netherlands, pp. 65–82

Baker NR, Oxborough K, Lawson T, Morison JI (2001) High resolution imaging of photosynthetic activities of tissues, cells and chloroplasts in leaves. J Exp Bot **52:** 615–621

Baker NR, Rosenqvist E (2004) Applications of chlorophyll fluorescence can improve crop production strategies: an examination of future possibilities. J Exp Bot **55:** 1607–1621

Baniulis D, Yamashita E, Whitelegge JP, Zatsman AI, Hendrich MP, Hasan SS, Ryan CM, Cramer WA (2009) Structure-function, stability, and chemical modification of the cyanobacterial cytochrome b6f complex from Nostoc sp. PCC 7120. J Biol Chem **284:** 9861–9869

Barbagallo RP, Oxborough K, Pallett KE, Baker NR (2003) Rapid, non-invasive screening for perturbations of metabolism and plant growth using chlorophyll fluorescence. Plant Physiol **132:** 485–493

Barkan A, Miles D, Taylor WC (1986) Chloroplast gene expression in nuclear, photosynthetic mutants of maize. EMBO J **5:** 1421–1427

Bernacchi CJ, Singsaas EL, Pimentel C, Portis AR Jr, Long SP (2001) Improved temperature response functions for models of Rubisco-limited photosynthesis. Plant Cell Environ **24:** 253–260

Björkman O, Demmig-Adams B (1994) Regulation of photosynthetic light energy capture, conversion, and dissipation in leaves of higher plants. *In* ED Schulze, MM Caldwell, eds, Ecophysiology of Photosynthesis. Springer-Verlag, Berlin, pp 17–47

Bruce BD, Malkin R (1991) Biosynthesis of the chloroplast cytochrome b6f complex: studies in a photosynthetic mutant of *Lemna*. Plant Cell 3: 203–212

Chida H, Nakazawa A, Akazaki H, Hirano T, Suruga K, Ogawa M, Satoh T, Kadokura K, Yamada S, Hakamata W, et al (2007) Expression of the algal cytochrome c6 gene in Arabidopsis enhances photosynthesis and growth. Plant Cell Physiol 48: 948–957

Clough SJ, Bent AF (1998) Floral dip: a simplified method for Agrobacterium-mediated transformation of Arabidopsis thaliana. Plant J 16: 735–743

Cramer WA, Zhang H (2006) Consequences of the structure of the cytochrome b6f complex for its charge transfer pathways. Biochim Biophys Acta 1757: 339–345

Cramer WA, Zhang H, Yan J, Kurisu G, Smith JL (2006) Transmembrane traffic in the cytochrome b6f complex. Annu Rev Biochem 75: 769–790

Driever SM, Simkin AJ, Alotaibi S, Fisk SJ, Madgwick PJ, Sparks CA, Jones HD, Lawson T, Parry MAJ, Raines CA (2017) Increased SBPase activity improves photosynthesis and grain yield in wheat grown in greenhouse conditions. Philos Trans R Soc B 372: 20160384

Ferreira KN, Iverson TM, Maghlaoui K, Barber J, Iwata S (2004) Architecture of the photosynthetic oxygen-evolving center. Science 303: 1831–1838

Fischer RA, Edmeades GO (2010) Breeding and crop yield progress. Crop Sci 50: S85–S98

Foyer CH, Neukermans J, Queval G, Noctor G, Harbinson J (2012) Photosynthetic control of electron transport and the regulation of gene expression. J Exp Bot 63: 1637–1661

Genty B, Briantais JM, Baker NR (1989) The relationship between the quantum yield of photosynthetic electron transport and quenching of chlorophyll fluorescence. Biochimica et Biophysica Acta 990: 87–92

Genty B, Goulas Y, Dimon B, Peltier JM, Moya I (1992) Modulation of efficiency of primary conversion in leaves, mechanisms involved at PSII. *In* N. Murata, ed, Research in Photosynthesis, Vol. 4, Kluwer Academic Publishers, Dordrecht, the Netherlands, pp. 603–610

Hager M, Biehler K, Illerhaus J, Ruf S, Bock R (1999) Targeted inactivation of the smallest plastid genome-encoded open reading frame reveals a novel and essential subunit of the cytochrome b(6)f complex. EMBO J 18: 5834–5842

Harrison EP, Willingham NM, Lloyd JC, Raines CA (1998) Reduced sedoheptulose-1,7-bisphosphatase levels in transgenic tobacco lead to decreased photosynthetic capacity and altered carbohydrate accumulation. Planta 204: 27–36

Hojka M, Thiele W, Tóth SZ, Lein W, Bock R, Schöttler MA (2014) Inducible repression of nuclear-encoded subunits of the cytochrome b_6f complex in tobacco reveals an extraordinarily long lifetime of the complex. Plant Physiol 165: 1632–1646

Hu X, Tanaka A, Tanaka R (2013) Simple extraction methods that prevent the artifactual conversion of chlorophyll to chlorophyllide during pigment isolation from leaf samples. Plant Methods 9: 19

Hurry V, Anderson JM, Badger MR, Price GD (1996) Reduced levels of cytochrome b 6/f in transgenic tobacco increases the excitation pressure on photosystem II without increasing sensitivity to photoinhibition in vivo. Photosynth Res 50: 159–169

Inskeep WP, Bloom PR (1985) Extinction coefficients of chlorophyll a and b in N,N-dimethylformamide and 80% acetone. Plant Physiol 77: 483–485

Jahns P, Holzwarth AR (2012) The role of the xanthophyll cycle and of lutein in photoprotection of photosystem II. Biochim Biophys Acta 1817: 182–193

Janik E, Bednarska J, Zubik M, Sowinski K, Luchowski R, Grudzinski W, Matosiuk D, Gruszecki WI (2016) The xanthophyll cycle pigments, violaxanthin and zeaxanthin, modulate molecular organization of the photosynthetic antenna complex LHCII. Arch Biochem Biophys 592: 1–9

Kamiya N, Shen JR (2003) Crystal structure of oxygen-evolving photosystem II from Thermosynechococcus vulcanus at 3.7-A resolution. Proc Natl Acad Sci USA 100: 98–103

Kaňa R, Kotabová E, Kopečná J, Trsková E, Belgio E, Sobotka R, Ruban AV (2016) Violaxanthin inhibits nonphotochemical quenching in light-harvesting antenna of *Chromera velia*. FEBS Lett 590: 1076–1085

Kanno K, Suzuki Y, Makino A (2017) A small decrease in Rubisco content by individual suppression of RBCS genes leads to the improvement of

photosynthesis and greater biomass production in rice under conditions of elevated CO_2. Plant Cell Physiol 58: 635–642

Kirchhoff H, Horstmann S, Weis E (2000) Control of the photosynthetic electron transport by PQ diffusion microdomains in thylakoids of higher plants. Biochim Biophys Acta 1459: 148–168

Knight JS, Duckett CM, Sullivan JA, Walker AR, Gray JC (2002) Tissue-specific, light-regulated and plastid-regulated expression of the single-copy nuclear gene encoding the chloroplast Rieske FeS protein of *Arabidopsis thaliana*. Plant Cell Physiol 43: 522–531

Kono M, Noguchi K, Terashima I (2014) Roles of the cyclic electron flow around PSI (CEF-PSI) and O_2-dependent alternative pathways in regulation of the photosynthetic electron flow in short-term fluctuating light in Arabidopsis thaliana. Plant Cell Physiol 55: 990–1004

Kramer DM, Avenson TJ, Kanazawa A, Cruz JA, Ivanov B, Edwards GE (2004) The relationship between photosynthetic electron transfer and its regulation. *In* GC Papageorgiou and Govindjee, eds, Chlorophyll a Fluorescence: A Signature of Photosynthesis, Springer, Dordrecht, the Netherlands. pp. 251–278

Kuras R, Wollman FA (1994) The assembly of cytochrome b6/f complexes: an approach using genetic transformation of the green alga *Chlamydomonas reinhardtii*. EMBO J 13: 1019–1027

Lefebvre S, Lawson T, Zakhleniuk OV, Lloyd JC, Raines CA, Fryer M (2005) Increased sedoheptulose-1,7-bisphosphatase activity in transgenic tobacco plants stimulates photosynthesis and growth from an early stage in development. Plant Physiol 138: 451–460

Lennartz K, Plücken H, Seidler A, Westhoff P, Bechtold N, Meierhoff K (2001) HCF164 encodes a thioredoxin-like protein involved in the biogenesis of the cytochrome b(6)f complex in *Arabidopsis*. Plant Cell 13: 2539–2551

Li XP, Björkman O, Shih C, Grossman AR, Rosenquist M, Jansson S, Niyogi KK (2000) A pigment-binding protein essential for regulation of photosynthetic light harvesting. Nature 403: 391–395

Li XP, Gilmore AM, Caffarri S, Bassi R, Golan T, Kramer D, Niyogi KK (2004) Regulation of photosynthetic light harvesting involves intrathylakoid lumen pH sensing by the PsbS protein. J Biol Chem 279: 22866–22874

Litvin R, Bina D, Vacha F (2008) Room temperature photooxidation of beta-carotene and peripheral chlorophyll in photosystem II reaction centre. Photosynth Res 98: 179–187

Loll B, Kern J, Saenger W, Zouni A, Biesiadka J (2005) Towards complete cofactor arrangement in the 3.0 A resolution structure of photosystem II. Nature 438: 1040–1044

Long SP, Marshall-Colon A, Zhu XG (2015) Meeting the global food demand of the future by engineering crop photosynthesis and yield potential. Cell 161: 56–66

López-Juez E, Jarvis RP, Takeuchi A, Page AM, Chory J (1998) New Arabidopsis *cue* mutants suggest a close connection between plastid- and phytochrome regulation of nuclear gene expression. Plant Physiol 118: 803–815

McMurtrie RE, Wang YP (1993) Mathematical models of the photosynthetic response of tree stands to rising CO_2 concentrations and temperature. Plant Cell Environ 16: 1–13

Metz JG, Miles D, Rutherford AW (1983) Characterization of nuclear mutants that lack the cytochrome f/b-563 complex. Plant Physiol 73: 452–459

Miles D (1982) The use of mutations to probe photosynthesis in higher plants. *In* E Edelman, RB Hallick, NH Chua, eds, Methods in Chloroplast Molecular Biology. Elsevier Biomedical Press, Amsterdam, pp 75–107

Miyagawa Y, Tamoi M, Shigeoka S (2001) Overexpression of a cyanobacterial fructose-1,6-/sedoheptulose-1,7-bisphosphatase in tobacco enhances photosynthesis and growth. Nat Biotechnol 19: 965–969

Monde RA, Zito F, Olive J, Wollman FA, Stern DB (2000) Post-transcriptional defects in tobacco chloroplast mutants lacking the cytochrome b_6/f complex. Plant J 21: 61–72

Müller P, Li XP, Niyogi KK (2001) Non-photochemical quenching: a response to excess light energy. Plant Physiol 125: 1558–1566

Murchie EH, Lawson T (2013) Chlorophyll fluorescence analysis: a guide to good practice and understanding some new applications. J Exp Bot 64: 3983–3998

Nakagawa T, Kurose T, Hino T, Tanaka K, Kawamukai M, Niwa Y, Toyooka K, Matsuoka K, Jinbo T, Kimura T (2007) Development of series of Gateway binary vectors, pGWBs, for realizing efficient construction of fusion genes for plant transformation. J Biosci Bioeng 104: 34–41

Oxborough K, Baker NR (1997a) An instrument capable of imaging chlorophyll a fluorescence from intact leaves at very low irradiance and at cellular and subcellular levels. Plant Cell Environ 20: 1473–1483

Oxborough K, Baker NR (1997b) Resolving chlorophyll *a* fluorescence images of photosynthetic efficiency into photochemical and nonphotochemical components: calculation of *qP* and *Fv/Fm* without measuring *Fo*. Photosynth Res **54**: 135–142

Price GD, von Caemmerer S, Evans JR, Siebke K, Anderson JM, Badger MR (1998) Photosynthesis is strongly reduced by antisense suppression of chloroplastic cytochrome bf complex in transgenic tobacco. Aust J Plant Physiol **25**: 445–452

Price GD, Yu JW, von Caemmerer S, Evans JR, Chow WS, Anderson JM, Hurry V, Badger MR (1995) Chloroplast cytochrome b6/f and ATP synthase complexes in tobacco: transformation with antisense RNA against nuclear-encoded transcripts for the Rieske FeS and ATP polypeptides. Aust J Plant Physiol **22**: 285–297

Raines CA (2006) Transgenic approaches to manipulate the environmental responses of the C3 carbon fixation cycle. Plant Cell Environ **29**: 331–339

Raines CA (2011) Increasing photosynthetic carbon assimilation in C3 plants to improve crop yield: current and future strategies. Plant Physiol **155**: 36–42

Ray DK, Ramankutty N, Mueller ND, West PC, Foley JA (2012) Recent patterns of crop yield growth and stagnation. Nat Commun **3**: 1293

Rosenthal DM, Locke AM, Khozaei M, Raines CA, Long SP, Ort DR (2011) Over-expressing the C(3) photosynthesis cycle enzyme Sedoheptulose-1-7 Bisphosphatase improves photosynthetic carbon gain and yield under fully open air CO_2 fumigation (FACE). BMC Plant Biol **11**: 123

Ruban AV (2012) The Photosynthetic Membrane: Molecular Mechanisms and Biophysics of Light Harvesting. Wiley-Blackwell, Oxford

Ruban AV, Lee PJ, Wentworth M, Young AJ, Horton P (1999) Determination of the stoichiometry and strength of binding of xanthophylls to the photosystem II light harvesting complexes. J Biol Chem **274**: 10458–10465

Ruban AV, Young A, Horton P (1994) Modulation of chlorophyll fluorescence quenching in isolated light harvesting complex of photosystem-II. Biochim Biophys Acta **1186**: 123–127

Ruban AV, Young AJ, Horton P (1996) Dynamic properties of the minor chlorophyll a/b binding proteins of photosystem II, an in vitro model for photoprotective energy dissipation in the photosynthetic membrane of green plants. Biochemistry **35**: 674–678

Ruuska SA, Andrews TJ, Badger MR, Price GD, von Caemmerer S (2000) The role of chloroplast electron transport and metabolites in modulating Rubisco activity in tobacco: insights from transgenic plants with reduced amounts of cytochrome b/f complex or glyceraldehyde 3-phosphate dehydrogenase. Plant Physiol **122**: 491–504

Schöttler MA, Flügel C, Thiele W, Bock R (2007) Knock-out of the plastid-encoded PetL subunit results in reduced stability and accelerated leaf age-dependent loss of the cytochrome b6f complex. J Biol Chem **282**: 976–985

Schöttler MA, Tóth SZ, Boulouis A, Kahlau S (2015) Photosynthetic complex stoichiometry dynamics in higher plants: biogenesis, function, and turnover of ATP synthase and the cytochrome b_6f complex. J Exp Bot **66**: 2373–2400

Schwenkert S, Legen J, Takami T, Shikanai T, Herrmann RG, Meurer J (2007) Role of the low-molecular-weight subunits PetL, PetG, and PetN in assembly, stability, and dimerization of the cytochrome b6f complex in tobacco. Plant Physiol **144**: 1924–1935

Simkin AJ, Lopez-Calcagno PE, Davey PA, Headland LR, Lawson T, Timm S, Bauwe H, Raines CA (2017) Simultaneous stimulation of sedoheptulose 1,7-bisphosphatase, fructose 1,6-bisphosphate aldolase and the photorespiratory glycine decarboxylase-H protein increases CO_2 assimilation, vegetative biomass and seed yield in Arabidopsis. Plant Biotechnol J **15**: 805–816

Simkin AJ, McAusland L, Headland LR, Lawson T, Raines CA (2015) Multigene manipulation of photosynthetic carbon assimilation increases CO_2 fixation and biomass yield in tobacco. J Exp Bot **66**: 4075–4090

Thayer SS, Björkman O (1992) Carotenoid distribution and deepoxidation in thylakoid pigment-protein complexes from cotton leaves and bundle-sheath cells of maize. Photosynth Res **33**: 213–225

Uematsu K, Suzuki N, Iwamae T, Inui M, Yukawa H (2012) Increased fructose 1,6-bisphosphate aldolase in plastids enhances growth and photosynthesis of tobacco plants. J Exp Bot **63**: 3001–3009

Vialet-Chabrand S, Matthews JSA, Simkin AJ, Raines CA, Lawson Y (2017) Importance of fluctuations in light on plant photosynthetic acclimation. Plant Physiol **173**: 2163–2179

von Caemmerer S, Farquhar GD (1981) Some relationships between the biochemistry of photosynthesis and the gas exchange of leaves. Planta **153**: 376–387

von Caemmerer S, Furbank RT (2016) Strategies for improving C4 photosynthesis. Curr Opin Plant Biol **31**: 125–134

Willey DL, Gray JC (1988) Synthesis and assembly of the cytochrome b-f complex in higher plants. Photosynth Res **17**: 125–144

Yamori W, Kondo E, Sugiura D, Terashima I, Suzuki Y, Makino A (2016) Enhanced leaf photosynthesis as a target to increase grain yield: insights from transgenic rice lines with variable Rieske FeS protein content in the cytochrome b6/f complex. Plant Cell Environ **39**: 80–87

Yamori W, Sakata N, Suzuki Y, Shikanai T, Makino A (2011a) Cyclic electron flow around photosystem I via chloroplast NAD(P)H dehydrogenase (NDH) complex performs a significant physiological role during photosynthesis and plant growth at low temperature in rice. Plant J **68**: 966–976

Yamori W, Takahashi S, Makino A, Price GD, Badger MR, von Caemmerer S (2011b) The roles of ATP synthase and the cytochrome b6/f complexes in limiting chloroplast electron transport and determining photosynthetic capacity. Plant Physiol **155**: 956–962

Yang XF, Wang YT, Chen ST, Li JK, Shen HT, Guo FQ (2016) PBR1 selectively controls biogenesis of photosynthetic complexes by modulating translation of the large chloroplast gene Ycf1 in Arabidopsis. Cell Discov **2**: 16003

Zapata M, Rodríguez F, Garrido JL (2000) Separation of chlorophylls and carotenoids from marine phytoplankton, a new HPLC method using a reversed phase C8 column and phridine-containing mobile phases. Mar Ecol Prog Ser **195**: 29–45

Zhu XG, Long SP, Ort DR (2010) Improving photosynthetic efficiency for greater yield. Annu Rev Plant Biol **61**: 235–261